Transportation Research Part C 144 (2022) 103908

Contents lists available at ScienceDirect

Transportation Research Part C

journal homepage: www.elsevier.com/locate/trc

Fine-grained crowd distribution forecasting with multi-order spatial interactions using mobile phone data

Mingxiao Li [a,b,c], Song Gao [b,*], Peiyuan Qiu [c,d], Wei Tu [a], Feng Lu [c,e,f], Tianhong Zhao [a], Qingquan Li [a]

[a] *Guangdong Key Laboratory of Urban Informatics, Shenzhen Key Laboratory of Spatial Information Smart Sensing and Services, and Research Institute of Smart Cities, School of Architeture & Urban Planning, Shenzhen University, Shenzhen 518060, China*
[b] *Geospatial Data Science Lab, Department of Geography, University of Wisconsin, Madison, WI 53706, USA*
[c] *State Key Laboratory of Resources and Environmental Information System, Institute of Geographic Sciences and Natural Resources Research, Chinese Academy of Sciences, Beijing 100101, China*
[d] *College of Surveying and Geo-Informatics, Shandong Jianzhu University, Jinan 250101, China*
[e] *University of Chinese Academy of Sciences, Beijing 100049, China*
[f] *The Academy of Digital China, Fuzhou University, Fuzhou 350002, China*

A R T I C L E I N F O

Keywords:
Crowd distribution forecasting
Multi-order spatial interaction
Embedding learning
Trajectory enhancement
Human mobility

A B S T R A C T

Fine-grained crowd distribution forecasting benefits smart transportation operations and management, such as public transport dispatch, traffic demand prediction, and transport emergency response. Considering the co-evolutionary patterns of crowd distribution, the interactions among places are essential for modelling crowd distribution variations. However, two issues remain. First, the lack of sampling design in passive big data acquisition makes the spatial interaction characterizations of less crowded places insufficient. Second, the multi-order spatial interactions among places can help forecasting crowd distribution but are rarely considered in the existing literature. To address these issues, a novel crowd distribution forecasting method with multi-order spatial interactions was proposed. In particular, a weighted random walk algorithm was applied to generate simulated trajectories for improving the interaction characterizations derived from sparse mobile phone data. The multi-order spatial interactions among contextual non-adjacent places were modelled with an embedding learning technique. The future crowd distribution was forecasted via a graph-based deep neural network. The proposed method was verified using a real-world mobile phone dataset, and the results showed that both the multi-order spatial interactions and the trajectory data enhancement algorithm helped improve the crowd distribution forecasting performance. The proposed method can be utilized for capturing fine-grained crowd distribution, which supports various applications such as intelligent transportation management and public health decision making.

Peer review under responsibility of Please add a footnote in the below mentioned format for all special issue papers with item group description as “VSI: <special issue title>”This article belongs to the Virtual Special Issue on “special issue full title”.

* Corresponding author.
E-mail address: song.gao@wisc.edu (S. Gao).

https://doi.org/10.1016/j.trc.2022.103908
Received 7 December 2021; Received in revised form 24 August 2022; Accepted 22 September 2022

1. Introduction

Fine-grained spatiotemporal crowd distribution forecasting is essential for traffic governance, urban management, and public health (Huang et al., 2021; Li et al., 2019a–c; Xu et al., 2018; Yao et al., 2020). For example, the department of traffic management can reschedule public transportation based on dynamic population distribution forecasting results to improve public travel efficiency; emergency management departments can forecast the crowd gathering processes of urban mass events, thereby improving the scientific nature and timeliness of control measures to reduce the risk of trampling (Chen et al., 2020; Iacobucci et al., 2019; Wang et al., 2019; Yuan & Raubal, 2016). Accurate crowd distribution forecasting can provide technical support and a decision-making basis for solving transportation problems and facilitating fine-grained traffic management, which is of great significance to the development of smart transportation.

Due to the lack of effective observation techniques, traditional urban mobility studies are mainly based on survey data, which limits the representativeness and spatiotemporal coverage of these studies (Zhang & Zhu, 2018; Chen et al., 2016). With the development of mobile positioning technology and the ubiquity of smart devices, long-time large-volume individual tracking data provide alternative opportunities for capturing the variation in human activities (Li et al., 2020; Yang et al., 2019; Gao et al., 2015; Gonzalez et al., 2008). In addition, breakthroughs in trajectory data mining and machine learning provide methodological support for urban mobility studies and applications (Ke et al., 2021; Liu et al., 2019; Park et al., 2019). They highlight the necessity of crowd distribution inference and forecasting (Li et al., 2021; Mimura et al., 2019; Chen et al., 2018).

With reference to the existing research on crowd distribution forecasting, two issues remain. First, the lack of sampling design in passive big data acquisition limits the accuracy and the stability of spatial interaction modelling. That is, the extracted spatial interaction pattern may significantly vary due to different sampling strategies and spatial heterogeneity in data distribution. This phenomenon is particularly evident in the less crowded places, which lead to the data hungry problem (Li et al., 2019; Yang et al., 2019). An example is shown in Fig. 1. Assuming that P_d is a place having 200 individuals at present, of which 130 individuals also stay in P_d at the previous time period moment and other 15, 50, and 5 individuals come from P_a, P_b, P_c, respectively. When the data were randomly sampled at 10 % of the population in each place, it may have resulted in oversampling of the individuals staying at P_d, while P_a and P_c, which originally had interactions with P_d, showed no interaction. This makes the spatial interaction characterizations of less crowded places insufficient, thereby reducing the accuracy of crowd distribution forecasting.

Second, the interactions among places cause crowd distribution variations, and these interactions can be reflected in individual movement trajectories (Peng et al., 2019; Zhu et al., 2018; Liu et al., 2017). The individual movement trajectories among multiple places portray the processes of crowd gathering and dispersing. These processes can be regarded as the multi-order spatial interactions among different places at the aggregation level. As far as we know, existing crowd forecasting studies often generalize trajectories as series of first-order interactions between two anchor places (origin–destination (OD) flows), thus ignoring the multi-order spatial interaction processes among the places (Li et al., 2021; Zhu et al. 2020). However, crowd distribution variation is influenced not only by contextual adjacent places (first-order interaction) but also by contextual non-adjacent places (multi-order interactions). For example, when one travels from home to work via a bus stop, if the entire movement trajectory is generalized and divided into the interaction between home and bus stop and the interaction between bus stop and work, the important multi-order/multi-context interactions between home and work will be ignored (Crivellari & Beinat 2019). Researches on multi-order spatial interaction learning can help model spatial correlations more comprehensively, thus improving the accuracy and interpretability of crowd distribution forecasting.

To address these issues, we proposed a novel **C**rowd **D**istribution **F**orecasting method with **M**ulti-order **S**patial **I**nteraction, called CDF-MSI, to forecast future crowd spatiotemporal distribution. The main contributions of this study are summarized as follows:

(1) A trajectory enhancement algorithm was applied to mitigate the problem of inaccurate interaction modelling in less crowded places caused by the lack of sampling design.
(2) The multi-order spatial interactions among contextual non-adjacent places were considered in the crowd distribution forecasting modelling to improve the forecasting accuracy and stability.
(3) A crowd distribution forecasting model was constructed using a hybrid graph-based deep neural network for modelling the spatiotemporal patterns of crowd distribution with multi-order spatial interactions.

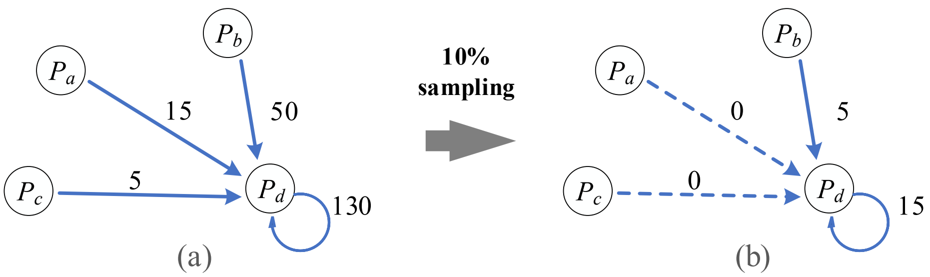

Fig. 1. An illustration of the spatial interaction pattern variation caused by data sampling.

(4) The performance of the proposed CDF-MSI method was evaluated with a real-world mobile phone dataset in Senegal. The results demonstrated the superiority of our proposed method over other baseline approaches.

The remaining parts of this paper are organized as follows. Section 2 presents a literature review on crowd distribution forecasting and its related studies. Section 3 presents the details of our proposed CDF-MSI method. Section 4 presents the experimental results and the performance analysis of the case study. Section 5 discusses the broad implications of this work and our vision for future work. Finally, Section 6 presents the conclusion of this study.

2. Literature review

2.1. Future crowd distribution forecasting

The urgent demand for forecasting future crowd distribution in applications such as public transport scheduling, emergency dispatch, mobile communication, and base station operations has promoted the development of crowd distribution forecasting research. According to the different aspects of attention, the existing methods can be divided into two categories: temporal variation pattern-based forecasting methods and spatial interaction pattern-based forecasting methods (Panczak et al., 2020).

Temporal variation pattern-based methods forecast future crowd distribution by modelling the temporal tendency and periodicity of the given crowd distribution variation sequence (Cecaj et al., 2020; Cheng et al., 2020; Mimura et al., 2019; Li et al., 2012). For example, Xue et al. (2020) proposed an expression method to reasonably divide a region and time period to determine the crowd distribution statistics and then designed an improved long short-term memory (LSTM) network to forecast future crowd distribution based on the temporal proximity, periodicity and trend characteristics. Mimura et al. (2019) designed a time series generation model based on conditional variational autoencoders and an LSTM network. It forecasts future crowd distribution by analysing the temporal variations in crowd distribution series and the influence of weather factors. Liang et al. (2016) designed a computational forecasting framework with parallel flow based on RNNs, which can effectively forecast near real-time crowd distribution by analysing the sequence characteristics of crowd size variations in a specific region. However, these methods only mine patterns from the historical time series of crowd distribution and ignore the effects of spatial interactions and spatial correlations, thus limiting their forecasting performance across space (Zhen et al., 2019; Shaw and Yu, 2009).

To address previous issues, researchers have started to forecast future crowd distribution by modelling the spatial interaction characteristics among places (Li et al., 2021; Crivellari & Beinat, 2019; Crols & Malleson, 2019; Chen et al., 2018). For example, Crols & Malleson (2019) applied a multi-agent model to characterize the commuting behaviours contained in travel survey data, thereby forecasting the crowd distribution by calibrating the difference between the distributions of commuters and urban populations based on Wi-Fi data. Chen et al. (2018) designed an artificial neural network to express the relationships between a historical crowd distribution and the inflow and outflow of people in each neighbourhood and forecasted the future crowd distribution in a large metropolitan area. On the basis of crowd movement behaviours in physical space, Li et al. (2021) integrated the interactions in physical spaces and social spaces with a graph fusion technique and forecasted the future crowd distribution by combining a GCN and a LSTM. However, most of the existing studies only consider first-order interaction characteristics (e.g., physical distances and OD flows) as the impact factors of crowd distribution forecasting. This makes the developed models fail to measure the influence of multi-order spatial interactions among contextual non-adjacent places on crowd distribution, resulting in insufficient forecasting accuracy and interpretability.

It is worth noting that the superiority of deep learning methods in capturing complex non-linear relationships has made it widely used in the field of traffic forecasting, such as traffic demand forecasting (Ke et al., 2021; Jin et al., 2020; Xu et al., 2017), traffic flow forecasting (Xu et al., 2022; Zhu et al., 2020; Zhang et al., 2020; Qiu et al., 2020), and traffic condition forecasting (Medrano & Aznarte, 2021; Zheng et al., 2020; Cui et al., 2019). For example, Ke et al. (2021) proposed a multi-task & graph learning approach to enable the knowledge of multiple kinds of service modes sharing across networks and designed various multi-graph convolutional networks for forecasting ride demands for different service modes. Zhang et al. (2020) regraded a road network as graphs for considering the topological structure of the underlying network and applied a GCN to forecast short-term traffic conditions. Geng et al. (2019) proposed a spatiotemporal multi-graph convolution network to capture the complicated spatiotemporal dependencies among different places and forecasted ride-hailing demand using a multi-graph integrated convolution technique. Li et al. (2017) designed a diffusion convolutional recurrent network for traffic flow forecasting by capturing the spatiotemporal dependency of traffic flows using bi-directional graph random walk and recurrent neural network with scheduled sampling. Solutions to these similar spatio-temporal forecasting problems provide reference and methodological foundation for crowd distribution forecasting. How to integrate deep learning methods and domain knowledge to improve the performance of crowd distribution forecasting is still a challenging problem worth exploring.

2.2. Historical crowd distribution mapping

The mapping of historical crowd distribution is the basis of crowd forecasting studies. Depending on the data sources used, the existing crowd distribution mapping methods can be divided into natural and socioeconomic data-based mapping methods, remote sensing image-based mapping methods, and geotagged data-based mapping methods.

The main idea of natural and socioeconomic data-based mapping methods is to quantitatively analyse the relationships between relevant factors and crowd distribution variations, thus assigning coarse-grained census data to fine-grained space (Leasure et al., 2020; Aryal, 2020; Krunić et al., 2015). Although this type of method has good spatial coverage and can improve the spatial granularity of crowd distribution mapping to a certain extent, it suffers from the problems of lagging data and a long update period. In addition, when combining natural and socioeconomic data with census data, problems such as temporal mismatches and inconsistencies across multiple statistical metrics affect the accuracy of crowd distribution mapping results.

Remote sensing image-based mapping methods mainly extract the features of relevant elements affecting crowd distribution through remote sensing images to establish relationships between the corresponding elements and crowd distribution variations. Common elements include the night-time lighting index, built-up area, etc. (You et al., 2020; Georganos et al., 2019). For example, Xing et al. (2020) proposed a deep learning architecture for learning the physical characteristics of remote sensing images and integrated neighbour effects to improve the crowd distribution mapping performance. Stathakis et al. (2018) assumed that the variations in observed night lights were a valid proxy for crowd distribution, thus estimating season-specific ambient crowd counts in Greece. This type of method significantly improves the spatial granularity and timeliness of prediction, but the acquisition of remote sensing data is limited by the given satellite transit time and weather conditions. This makes the mapping results of these methods unable to capture the dynamic processes of fine-grained population distributions (e.g., hourly) and suffers from missing data problems.

With the decreasing data collection cost, the geotagged data-based mapping method has become mainstream in historical crowd distribution mapping. Emerging methods focus on taxi trajectories, social media data or smart card data (Hara et al., 2020; Hipp et al., 2018; Wang et al., 2018). However, the sample biases in these data make the mapping results suffer from representativeness problems (Mellon & Prosser, 2017). Since mobile phone data cover almost all classes of the population and have fine spatiotemporal granularity, they have become one of the main data sources for historical crowd distribution mapping (Salat et al., 2020; Li et al., 2020; Liu et al., 2018; Deville et al, 2014). Kang et al. (2012) quantitatively analysed the correlations among the number of calls, the number of active mobile phone users, and the size of the associated crowd, thus demonstrating the linear relationships between crowd distribution and mobile phone indicators. Cheng et al. (2020) mapped monthly crowd distribution across China using mobile phone data and environmental ancillary data through a hybrid method containing a random forest model and area-to-point interpolation. The importance measures of the explanatory variables in this method demonstrated the ascendancy of mobile phone data in crowd distribution mapping. However, since most mobile phone data only record the corresponding location when communication or transition behaviour occurs, mobile phone data suffer from the data sparsity problem (Li et al., 2019; Chen et al., 2019). In addition, the lack of corresponding attribute values (e.g., age, gender, etc.) in mobile phone data limits the application of crowd distribution mapping results to a certain extent.

2.3. Spatial interaction pattern analysis

Spatial interaction refers to the phenomenon of the movement or exchange of people, objects or information that occurs among places (Tobler, 1976). It reveals the connections among places, which provides great support for research on crowd distribution variation (Ullman, 1953; Park et al., 2018).

Limited by data availability, traditional spatial interaction intensity estimation methods mostly regard places as nodes and construct mechanistic models to estimate spatial interaction intensity. The most common models include the gravity model, intervening opportunities model, and random walk model. For example, the gravity model draws on the idea of the law of gravity, which suggests that the intensity of spatial interaction is proportional to regional attributes (population, gross domestic product, etc.) and decays with increasing inter-regional distance (Zipf, 1946). The gravity model is widely used in many fields, such as population migration and international trade; however, it has certain shortcomings in practical applications due to its reliance on historical data calibration for parameter setting and the need for a priori knowledge to perform distance function selection (Gupta et al., 2019; Park et al., 2018). The intervening opportunities model introduced the principle of maximum entropy instead of spatial distance to explain spatial interaction intensity, which reflects the decision processes of human travel behaviours in the original hypothesis (Stouffer, 1940). However, this model has problems such as an overcomplicated solution process and the underestimation of long-distance travel proportions. Simini et al. (2012) regarded a spatial interaction as a random process determined by a joint probability, which was determined by the crowd distribution of the origin, destination and calculation radius. This model makes it possible to estimate spatial interaction intensities by only inputting the crowd distribution, thereby solving the cold start problem of spatial interaction intensity estimation models.

Different from the above mechanistic model, the quick accumulation of geotagged data enables us to estimate and forecast the intensities of the spatial interactions among places from a data-driven perspective (Ouyang et al., 2020; Wu et al., 2018). For example, Zhang et al. (2017) designed a deep spatio-temporal residual network (ST-ResNet) to forecast spatial interaction intensities by modelling the spatial dependence and the proximity, periodicity, and trend characteristics of the input spatial interaction intensity sequences. Wu et al. (2018) introduced an attention mechanism based on convolutional and RNN models by automatically learning the historical importance of spatial interaction intensities to further improve the accuracy of spatial forecasting. It is worth noting that the generation of spatial interactions is related to the selection of human movement behaviours, and this selection process is directly reflected in human movement trajectories (Zhang et al., 2021; Liu et al., 2020). The learning of interaction patterns among multiple places based on trajectory data will help us understand the mechanisms of human movement behaviours, measure the spatial correlations among places more comprehensively, and then improve the accuracy and interpretability of crowd distribution forecasting.

3. Methodology

The details of our proposed crowd distribution forecasting method are presented in this section. It contains three parts. First, the weighted random walk algorithm used in this study for trajectory data enhancement is introduced to improve the interaction characterization performance in less crowded places. Then, an embedding learning technique is introduced for learning the multi-order interactions among different places. Finally, the architecture of the proposed crowd distribution forecasting model is presented. The overall framework is shown in Fig. 2.

3.1. Trajectory data enhancement

Due to the lack of sampling design in passive trajectory data acquisition, the extracted spatial interaction pattern may significantly vary. This makes the spatial interaction characterizations of less crowded places especially insufficient, thereby reducing the accuracy of crowd distribution forecasting. To mitigate this issue, a weighted random walk algorithm was used to generate simulated trajectories which started at less crowded places for trajectory data enhancement.

To minimize the difference between the simulated trajectories and real trajectories, we represent the interaction patterns reflected in the input historical trajectories as a directed and weighted graph for trajectory simulation. In this graph, the places were represented as nodes, and the number of interaction records between two places was taken as the edge weight. An illustration of the interaction graph is shown in Fig. 3, where $w_{i,j}$ represents the number of interaction records from a place S_i to another S_j, and an interaction was detected when the two adjacent trajectory records of one individual were linked to different places.

Combined with the generated interaction graph, trajectory simulation can be regarded as a weighted random walk process. In this study, a second-order random walk algorithm was introduced for trajectory data enhancement (Grover & Leskovec, 2016). Different from the simple weighted random walk algorithm that simulates the next visit place based on the current place S_t and the edge weight $w_{t,j}$, our second-order algorithm also considered the effects of the previously visited place S_{t-1} to further minimize the difference between the simulated trajectories and real trajectories. The simulation process can be briefly explained as follows. Given the current place S_m and the previously visited place S_l that an agent has visited, the probability of visiting the next place S_n can be defined as

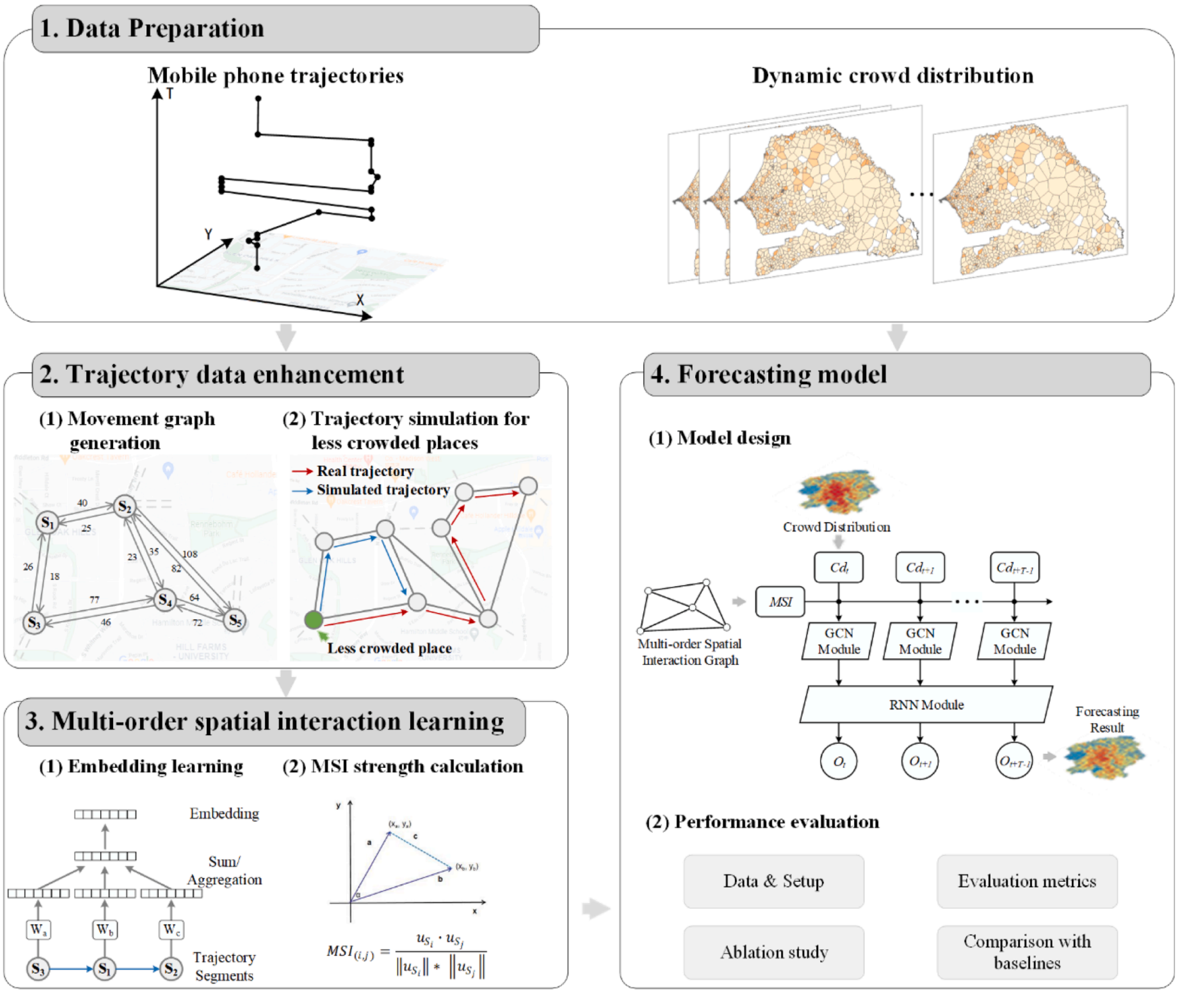

Fig. 2. The overall framework of the CDF-MSI method.

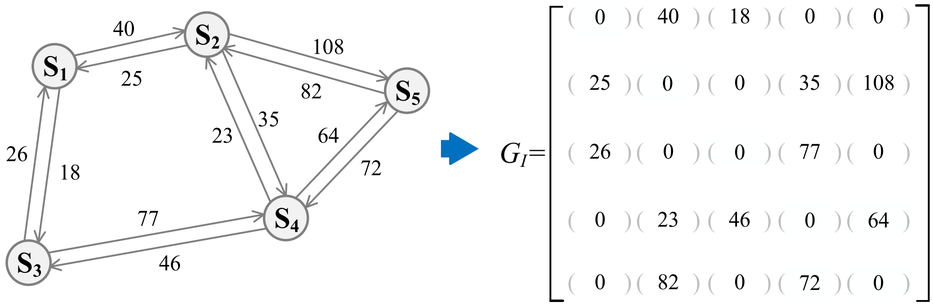

Fig. 3. An illustration of interaction graph generation.

follows:

$$P(S_{t+1} = S_n | S_t = S_m) = \alpha_{(l,n)} {}^{*} w_{m,n} / Z \tag{1}$$

$$\alpha_{(l,n)} = \begin{cases} 1/p, if\, d_{l,n} = 0 \\ 1, if\, d_{l,n} = 1 \\ 1/q, if\, d_{l,n} = 2 \end{cases} \tag{2}$$

where P indicates the visit probability, $w_{m,n}$ indicates the corresponding edge weight in the interaction graph, Z indicates the standardized coefficients, and $d_{l,n}$ indicates the minimum number of edges between places S_l and S_n. Parameter p controls the likelihood of revisiting nodes in the walk, and a high value of this parameter ensures a lower probability of visiting a visited place; parameter q controls the search to move in the "inward" or "outward" direction, and a high value of this parameter ensures a lower probability of visiting places close to S_l. The parameters p and q can be calibrated based on the movement pattern of the real trajectories which were tuned as 0.25 and 2 in this case study. Based on the proposed weighted random walk algorithm, the less crowded places were chosen as start nodes, and simulated trajectories were generated for trajectory data enhancement. The generated simulation trajectories and the real trajectories will be used as inputs for subsequent multi-order spatial interaction learning together to enhance the effectiveness of spatial interaction characterization. It is worth noting that the generated simulation trajectories in less crowded places were only used for learning the spatial interaction pattern among places (i.e., the underlying connectivity and spatial structure of places) and were not used in the crowd distribution estimation. The crowd distribution was only obtained from the real trajectories.

3.2. *Multi-order spatial interaction learning*

The movements of individuals among different locations/places can cause crowd distribution variations. As a microscopic part of an urban system, the individual movement behaviours recorded in the trajectory data provide a feasible idea for measuring the multi-order spatial interaction characteristics of places. Inspired by the achievements in computational linguistics, we regarded the trajectories as text sequences, thereby introducing an embedding learning technique to characterize the multi-order interactions among places (Zhang et al., 2021).

As the word2vec model can effectively extract the co-occurrence relationships and common context relationships among words in text, it has become a popular embedding learning technique. The core idea of this model is to express words as N-dimensional vectors and make a vector of words with more co-occurrences and common context relationships that are more similar. Therefore, the semantic relevance among words can be measured through vector similarity. Considering the data structure similarity between trajectory and text sequences, we used this model to characterize the multi-order interactions among places. An illustration of the places

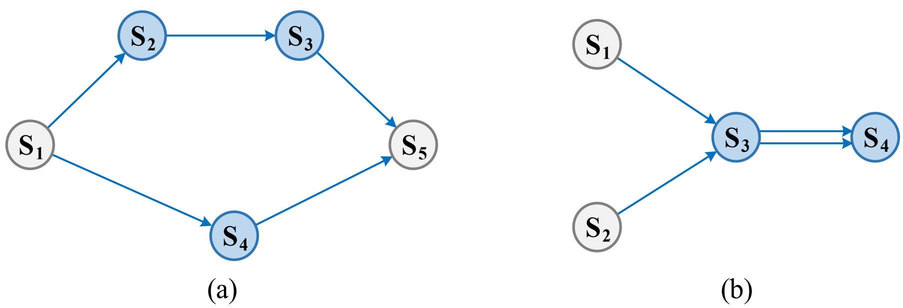

Fig. 4. An illustration of places that (a) share a common context or (b) frequently co-occur. The places labelled in blue have high spatial correlations. (For interpretation of the references to colour in this figure legend, the reader is referred to the web version of this article.)

with common context and co-occurrence relationships is shown in Fig. 4. As shown in Fig. 4(a), the places S_2, S_3, and S_4 have common upstream and downstream neighbours S_1 and S_5, indicating that these places have common context relationships. Correspondingly, the places S_3 and S_4 in Fig. 4(b) appear in two trajectory segments $<S_1, S_3, S_4>$ and $<S_2, S_3, S_4>$, indicating that these places have co-occurrence relationships. The places with either common context or co-occurrence relationships have high spatial correlations, thus justifying the usage of the word2vec model for multi-order spatial interaction learning.

The training process can be briefly summarized as follows. Given an enhanced trajectory $Traj_k = S_1, S_2, \cdots, S_H$, the core idea is to maximize the average log probability:

$$\frac{1}{H}\sum_{h=1}^{H}\sum_{k=-K}^{K}\log P(S_{t+k}|S_t) \tag{3}$$

where K indicates the number of spatial interaction orders considered in the model. $P(S_{t+k}|S_t)$ indicates the probability of correctly forecasting visit place S_{t+k} given current place S_t, and this probability is defined as follows:

$$P(S_{t+k}|S_t) = \frac{\exp\left({u'_{S_{t+k}}}^{T} u_{S_t}\right)}{\sum_{v=1}^{V}\exp\left({u'_{S_v}}^{T} u_{S_t}\right)} \tag{4}$$

where V indicates the number of places and u'_{S_v} and u_{S_v} indicate the initial one-hot vector and the trained N-dimensional vector of the place, respectively. The training process typically uses the back-propagation rule (Rumelhart et al., 1986). More technical details can be found in the paper (Mikolov et al., 2013). It is worth noting that only trajectories from the training data were used to learn the multi-order spatial interaction to avoid overfitting phenomena.

With the trained model, each place can be expressed as an N-dimensional vector. Therefore, the multi-order spatial interaction graph can be calculated by the similarity between each pair of trained vectors as follows:

$$MSI_{(i,j)} = \frac{u_{S_i} \bullet u_{S_j}}{\|u_{S_i}\| * \|u_{S_j}\|} \tag{5}$$

where $MSI_{(i,j)}$ indicates the multi-order spatial interaction strength between places S_i and S_j, and $\|u_{S_i}\|$ and $\|u_{S_j}\|$ represent the norms of trained vectors u_{S_i} and u_{S_j}, respectively. A higher $MSI_{(i,j)}$ value indicates that the two places more frequently co-occur or share common contexts in the trajectories, that is, a higher multi-order interaction strength between the two places.

3.3. Forecasting model with a graph-based deep neural network

Based on the multi-order spatial interaction graph, a graph-based deep neural network model was designed for crowd distribution forecasting. The architecture of this model can be summarized in two parts: the characterization of the multi-order spatial interaction pattern of the crowd distribution with a GCN module and the characterization of the temporal variation pattern of the crowd distribution with an RNN module. An illustration of the CDF-MSI model is shown in Fig. 4.

As shown in Fig. 5, the current crowd distribution Cd_t and the multi-order spatial interaction matrix MSI were first organized into graph form as the model input. Specifically, the places were abstracted as nodes, the crowd distribution Cd_t was abstracted as node weights, and MSI was abstracted as edge weights. It is worth noting that the MSI matrix should be transformed into a Laplacian matrix

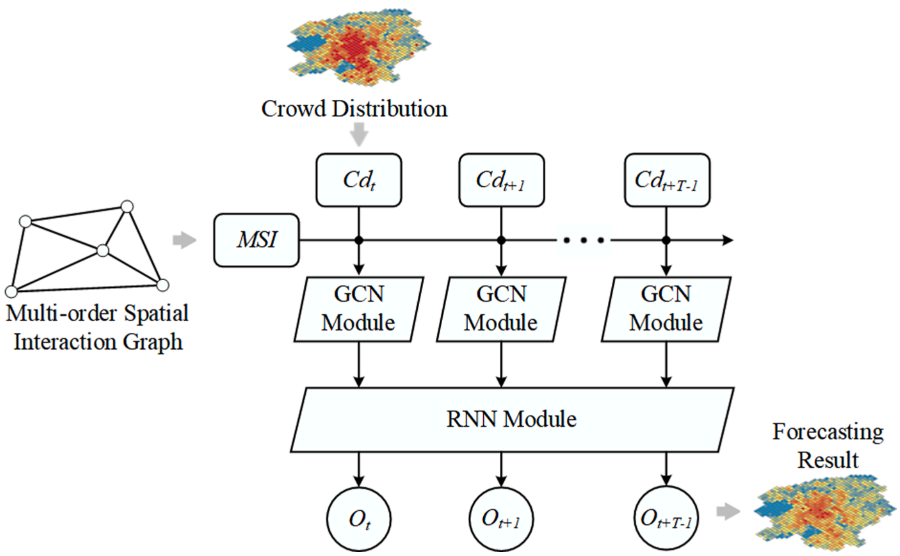

Fig. 5. The architecture of the CDF-MSI model.

for fitting the input of the GCN (Kipf & Welling, 2016). Based on the transformed *MSI* matrix, a GCN module was applied for modelling the spatial variation pattern of the crowd distribution, which can be calculated as follows:

$$Cd_t^{r+1} = \in(MSI^{'}*Cd_t^r*W_t^r) \tag{6}$$

where Cd_t^r represents the feature matrix (which equals Cd_t when the number of convolutions r equals one), $\in$ represents the activation function, $MSI^{'}$ represents the multi-order spatial interaction matrix *MSI* changed by the Laplace transform, and W_t^r represents the weight matrix for model training.

On the basis of the GCN module, an RNN module was then used as the encoding–decoding framework for modelling the temporal variation pattern of the crowd distribution. During this process, a time step T was first determined with the temporal autocorrelation function (Cheng et al., 2020). According to the determined time step, the feature matrices $Cd_t^{r+1}, Cd_{t+1}^{r+1}, \ldots, Cd_{t+T-1}^{r+1}$ were organized into time series and inputted into the RNN module. An LSTM architecture was used in our method and the corresponding formulas are shown as follows:

$$z_t^g = \sigma(W^g*[Cd_t^{r+1}, h^{t-1}] + b^g) \tag{7}$$

$$\widetilde{C}_t = \tanh(W^c*[Cd_t^{r+1}, h^{t-1}] + b^c) \tag{8}$$

$$C_t = z_t^f*C_{t-1} + z_t^i*\widetilde{C}_t \tag{9}$$

$$h_t = z_t^o*\tanh(C_t) \tag{10}$$

where Cd_t^{r+1} represents the trained result of GCN module, z_t^g represents the gate state at time t, $g \in [f, i, o]$ indicate the forget gate, input gate, and output gate, respectively. C_t and h_t represent the cell state and the current output at time t, $\widetilde{C}_t$ represents the candidate values that could be added to cell state. W^g and W^c represent the corresponding weight matrix, and b^g and b^c represent the corresponding bias. The minimum root mean square error (RMSE) of the forecasted crowd distribution was used as the optimization criterion for model training. With this architecture, the CDF-MSI model was trained to forecast future crowd distribution. When performing forecasting, the new crowd distribution matrix sequence and the multi-order spatial interaction strength matrix were passed into the trained model, and then the forecasting results of the crowd distribution were obtained.

4. Case study

4.1. Data and experiment setup

The data used in this study were obtained from an anonymized mobile phone dataset provided by a major telecom operator in Senegal. It contains over 300,000 of individuals for one year in 2013. The dataset was accessed through the "Data for Development" challenge (De Montjoye et al. 2014). The data we used were the individual trajectories extracted from the call detail records of 10 % of the sampled users. An example from this dataset is shown in Table 1. It is worth noting that all personal information was deleted before the data were provided due to personal privacy concerns. The data whose numbers of active days were<25 % of the total days or whose numbers of records were larger than 1000 were deleted in the data pre-processing. Accordingly, as the number of users was generally linearly proportional to the size of the crowd (Kang et al., 2012), the catchment area of the cell phone tower was regarded as the place (the study unit) and the number of records of each tower was aggregated in hourly intervals to represent the crowd distribution for model evaluation (the detailed calculation process referred to the papers (Wang et al., 2018; Niu et al., 2015)). For performance evaluation, the last 10 % day's data were used as test data, the last 10 % of the remaining data was used as validation data, and the others were used as training data. A map of the crowd distribution in Senegal was shown in Fig. 6.

The parameters used in this case study are shown in Table 2. The parameters were mainly tuned according to the grid search strategy based on the lowest obtained RMSE value on the validation dataset (Chai et al., 2018). The simulated trajectory length was tuned to 22, which corresponded to the weekly average length of the real individual trajectories. The less crowded places in this paper were defined as the places with the total crowd count in the bottom 20 % of all places. It was inspired by the Pareto principle (Sanders, 1987), and the specific value was 48 in this study. The less crowded places were chosen as start nodes for trajectory data enhancement until the average count of individuals in this place reached the less crowded threshold. The spaces of parameters can be calibrated based on the individual movement pattern and the crowd distribution pattern (Li et al., 2020).

Table 1
Examples of individual trajectory data extracted from call detail records.

Individual ID	Date	Time	Tower ID	Longitude	Latitude
4607****	01–07	0:20	164	−17.45**	14.74**
4607****	01–07	10:10	88	−17.46**	14.74**
4607****	01–07	10:50	134	−17.46**	14.75**
4607****	…	…		…	…
4607****	01–20	21:10	143	−17.45**	14.74**

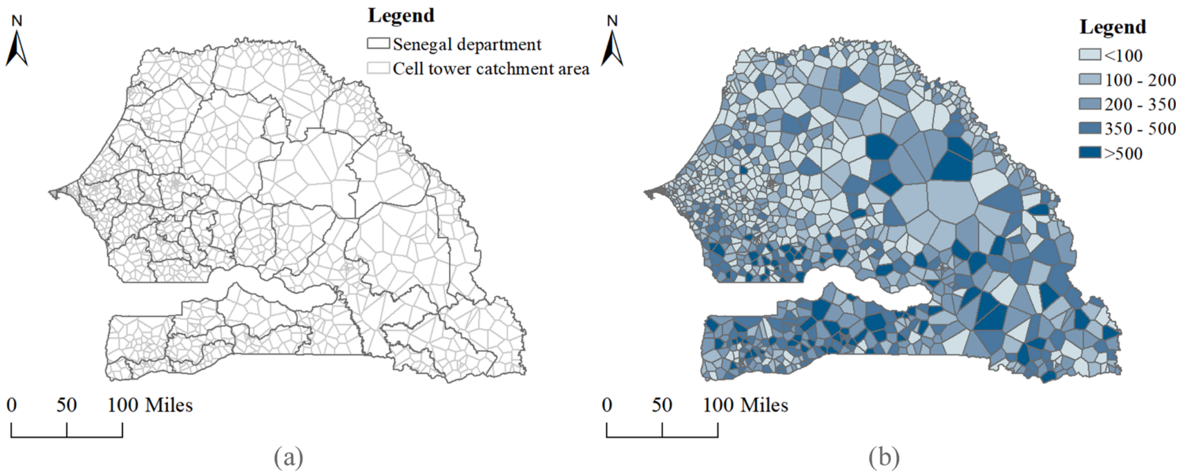

Fig. 6. The maps of (a) the case study area, and (b) the crowd distribution based on mobile phone data.

Table 2
Parameters used in this study.

Parameter	Value	Parameter	Value
Multi-order size	9	GCN layers	1
Simulated trajectory length	22	Convolution kernel size	1
Less crowded threshold	48	LSTM layers	1
Number of hidden units	64	Time step	6

4.2. Evaluation metrics

The RMSE, MAE and StDev metrics were used to evaluate the forecasting errors and the stability of the forecasting methods. Given the crowd distribution of all cell phone towers at time t $C_t = c_{1,t}, c_{2,t}, \cdots, c_{V,t}$ and the forecasted crowd distribution $C_t^{'} = c_{1,t}^{'}, c_{2,t}^{'}, \cdots, c_{V,t}^{'}$, the evaluation metrics can be defined as follows:

$$RMSE = \sqrt{\frac{\sum_{t=1}^{T}\sum_{v=1}^{V}\left(c_{v,t} - c_{v,t}^{'}\right)^2}{V*T}} \tag{11}$$

$$MAE = \frac{\sum_{t=1}^{T}\sum_{v=1}^{V}\left|c_{v,t} - c_{v,t}^{'}\right|}{V*T} \tag{12}$$

$$StDev = \sqrt{\frac{\sum_{t=1}^{T}\sum_{v=1}^{V}\left(\left(c_{v,t} - c_{v,t}^{'}\right) - \overline{Error}\right)^2}{V*T-1}} \tag{13}$$

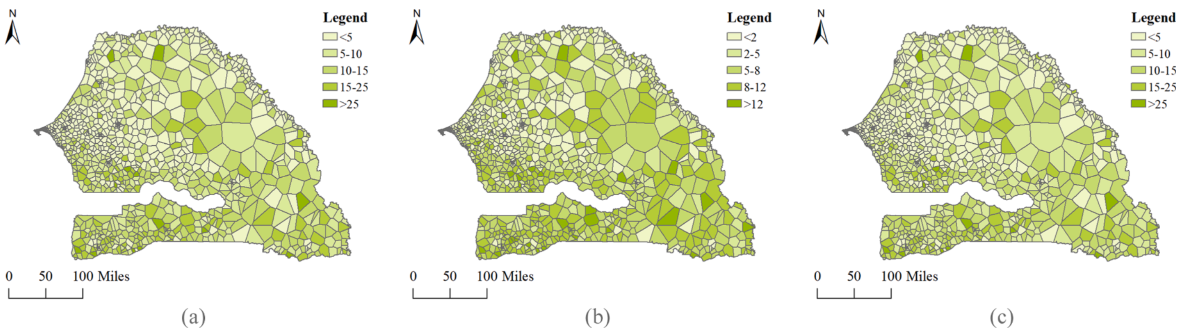

Fig. 7. The forecasting performance of the CDF-MSI method in terms of the (a) RMSE, (b) MAE, and (c) StDev.

where V represents the number of cell phone towers, T represents the number of time slots needed to be forecasted, and $\overline{Error}$ represents the average of all forecasting errors. The maps of the average forecasting performance (RMSE and MAE) and forecasting error deviation (StDev) with respect to each place are shown in Fig. 7.

4.3. Comparison of the CDF-MSI method with baselines

To evaluate the performance of our proposed CDF-MSI method relative to that existing crowd distribution forecasting methods using machine learning, the following five methods were selected as baselines. For all methods, the parameters were tuned with a grid search algorithm based on the performance on the validation dataset. The detailed parameters of baselines were attached in Table S1 in the supplement file. To test the stability of the forecasting performance, each method was run ten times repeatedly. The average of ten results was used to indicate the average predictive performance of each model, and the best result of each method was used for subsequent analysis.

- **Spatio-Temporal meta-Model (STMeta):** This model integrated generalizable spatiotemporal knowledge with multi-view learning and predicted the crowd flows by combining graph convolution LSTM and attention mechanism (Wang et al., 2020).
- **Diffusion Convolutional Recurrent Neural Network (DCRNN):** This model captured the spatiotemporal dependency of traffic flows by using bi-directional graph random walk and recurrent neural network with scheduled sampling (Li et al, 2017).
- **Attention based Spatial-Temporal GCN (ASTGCN):** This model applied a spatiotemporal attention mechanism to model the autocorrelations within the crowd distribution and capture the spatiotemporal variation patterns by combining a GCN and a standard convolutional network (Guo et al., 2019).
- **LSTM:** This model is one of the most advanced recurrent deep learning techniques used in time series data modelling. It has been widely used in similar forecasting tasks such as traffic flow forecasting and next location forecasting. (Ren et al., 2020; Li et al., 2020).
- **K-Nearest Neighbours (KNN):** This model splits the crowd distribution sequences into fixed-length sub-sequences and finds the k samples that are most similar to the forecasted sequence. The average value or weighted average value of the k samples was outputted as the forecasting result (Smith et al., 2002).
- **Gradient-Boosting Decision Tree (GBDT):** The GBDT model regards fixed-length crowd distribution sub-sequences as features and trains a model with an iterative decision tree generation algorithm. The results of all trained decision trees are added as the forecasting result (Friedman, 2001).

The comparison results are shown in Table 3. The best RMSE and MAE of our proposed CDF-MSI method were 8.885 and 4.633, respectively, thus outperforming all other baseline methods. The StDev of the CDF-MSI method was also the lowest, indicating that our proposed method showed an advantage regarding the stability of the forecasting error. Considering the sensitivity of the RMSE to outliers, the RMSE was used as the major evaluation metric in subsequent analysis (Chai & Draxler, 2014). We observed that the deep learning-based methods, including CDF-MSI, STMeta, DCRNN, ASTGCN, and LSTM, outperformed the classical machine learning-based methods. This phenomenon can be explained by the fact that deep learning-based methods better capture non-linear and complex spatiotemporal variation patterns. The spatiotemporal methods (CDF-MSI, STMeta, DCRNN, and the ASTGCN) showed better forecasting performance than the temporal methods (LSTM, KNN, and the GBDT), which may demonstrate the necessity of considering spatial patterns in the crowd distribution forecasting problem. It is worth noting that the RMSE and StDev values were not significantly different. This is mainly because some of the forecasting errors were positive and some were negative, making the average forecasting error $\overline{Error}$ (as shown in Formula 13) approximately equal to zero. However, these are two different aspects of the metrics used to evaluate the forecasting error and the stability of the forecasting error.

A significance test was further conducted to verify the significance of the forecasting performance differences between the CDF-MSI method and the other baseline methods. Considering that the forecasting errors did not conform to a Gaussian distribution, the Kolmogorov-Smirnov test (K-S test) was chosen as the indicator. As shown in Table 4, all compared pairs achieved larger K-S statistic values than the expected values of the null hypothesis, and the p-values were <0.001. The results indicate that the forecasting errors of CDF-MSI were significantly different from those of the other methods, thus demonstrating the effectiveness of our proposed method.

Table 3
Performance comparison with baselines.

Category	Method	RMSE		MAE		StDev	
		Mean	Best	Mean	Best	Mean	Best
Deep Learning	**CDF-MSI**	**8.894**	**8.885**	**4.643**	**4.633**	**8.893**	**8.884**
	STMeta	10.817	10.809	5.910	5.902	10.784	10.777
	DCRNN	9.749	9.741	5.388	5.380	9.675	9.667
	ASTGCN	9.941	9.933	4.715	4.703	9.928	9.920
	LSTM	29.462	29.458	4.907	4.880	29.450	29.446
Classical Machine Learning	GBDT	46.875	46.874	6.588	6.576	46.858	46.856
	KNN	47.241	47.241	7.141	7.141	47.222	47.222

Table 4
The Kolmogorov-Smirnov test results for the forecasting error comparison.

Compared pairs	K-S statistics	p-values
CDF-MSI & STMeta	0.1808	$p < 0.001$
CDF-MSI & DCRNN	0.2173	$p < 0.001$
CDF-MSI & ASTGCN	0.0345	$p < 0.001$
CDF-MSI & LSTM	0.2270	$p < 0.001$
CDF-MSI & KNN	0.0829	$p < 0.001$
CDF-MSI & GBDT	0.0864	$p < 0.001$

To further demonstrate the advantage of our proposed CDF-MSI method, the forecasting performance was evaluated in terms of the size of the crowd and the diversity of the crowd variations.

As discussed previously, the forecasting performance varies for places with different levels of congestion. With reference to Senegal's urbanization rate of approximately 40 %, we classified the places into three groups with crowd size thresholds of 195 and 435 (World bank, 2014). The thresholds corresponded to cumulative distribution values of 60 % and 90 % with respect to the size of the crowd statistical distribution, roughly dividing the case study area into rural areas, township areas, and urban areas. The comparison results are shown in Fig. 8. We observed that the forecasting performance decreased with increasing crowd size. It was to be expected that the less crowded places led to simpler variation patterns and lower forecasting difficulty. Note that although the RMSE of our proposed CDF-MSI method increased from 4.647 to 16.620, but it still achieved good performance among the compared methods.

The diversity of the crowd variations in the places affects the forecasting performance from another perspective. In this study, the standard deviation of the crowd size over the time series in a place was used to evaluate the stability and complexity of crowd size variations. Correspondingly, the division thresholds were chosen as 35 and 95, representing cumulative distribution values of 60 % and 90 %, respectively, in terms of the diversity of the statistical distribution of the crowd variations in places. The comparison results are shown in Fig. 9. All the comparison methods achieved good forecasting performance when the crowd variation diversity was simple. Note that the differences in forecasting performance between our proposed CDF-MSI method and the classical machine learning methods for both the small crowd size group and simple variation group were small. This result indicates that the complex methods tended to be more significantly improved when solving complex problems. Nevertheless, our method still performed well for each group.

4.4. Evaluation of the two algorithms in the CDF-MSI method

As mentioned in the methodology section, a trajectory enhancement algorithm and a multi-order spatial interaction learning algorithm were applied in the CDF-MSI method to achieve forecasting performance improvement. To verify the applicability of these two algorithms on performance improvement, three strategies were designed for performance evaluation: (1) models with the trajectory enhancement part and the multi-order spatial interaction learning (with suffix -MSI), (2) models with the multi-order spatial interaction learning algorithm only (with suffix -OMSI), and (3) models with the first-order interaction as edge weights only (with suffix -FI). In addition, to verify the applicability of these two algorithms on performance improvement, the spatiotemporal deep graph neural network models, including MSI, STMeta, DCRNN, and ASTGCN, were used as basic models for the ablation study. The adjacency matrices generated by the above three strategies were input into the corresponding basic models for model training. The evaluation results were shown in Fig. 10. The results showed that the models with both algorithms achieved better forecasting performance than the others. Specifically, the models with suffix -MSI performed better than the models with suffix -OMSI, indicating that the trajectory enhancement algorithm (fixing the issue of insufficient interaction sampling in less crowded places) was helpful for achieving better

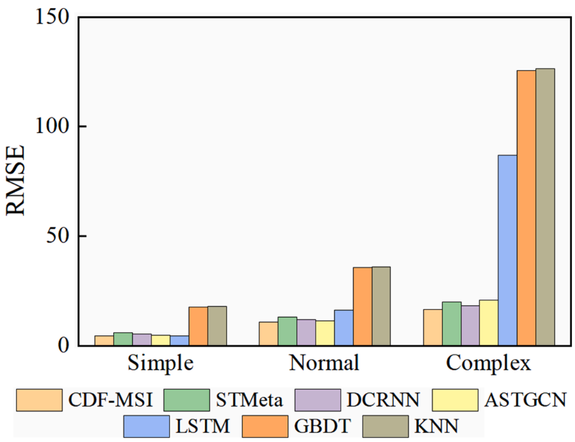

Fig. 8. Effect of crowd size on the RMSE.

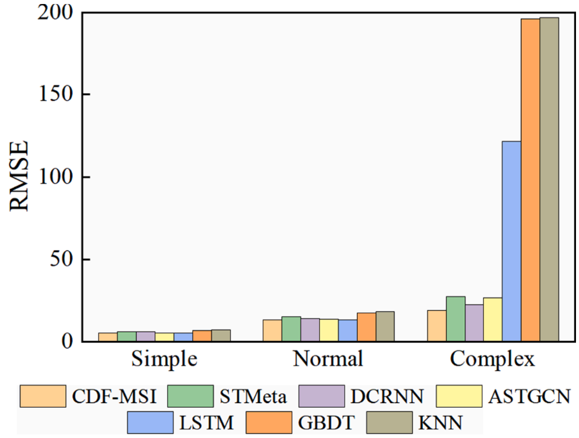

Fig. 9. Effect of crowd variation diversity on the RMSE.

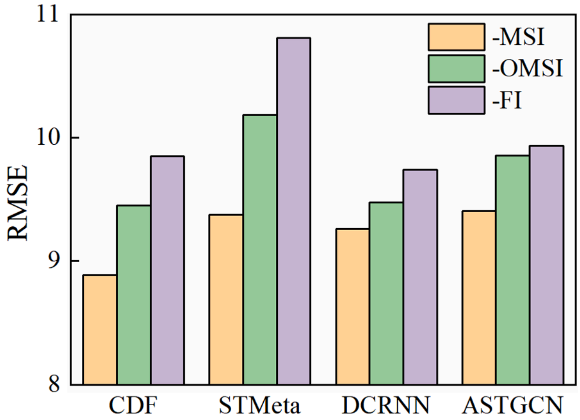

Fig. 10. Verification of the applicability of these two algorithms on performance improvement.

forecasting performance. Both the models with suffix -MSI and -OMSI outperformed other models, indicating that the multi-order spatial interaction learning algorithm also contributed to the improvement in forecasting performance. These results demonstrated the advantage of the two algorithms proposed in this paper to a certain extent.

As for the trajectory enhancement algorithm, the 2nd-order random walk with historical movement interaction was used to generate simulated trajectories in this study. To test the similarity between the simulated trajectories and the real trajectories, a simulated trajectory dataset was generated. The number of generated trajectories originated from each place is equal to its average population count observed from the mobile phone data. The Pearson correlation was chosen as the evaluation metric, and the perspectives of average number of stay points per place, the median trajectory entropy per place, the crowd distribution, and the movement interaction matrix, were chosen to measure the similarity between the real trajectories and the simulated trajectories (Wang et al., 2019). The results were shown in Table 5. The correlation coefficients between the simulation trajectories and real trajectories in all four perspectives were over 0.8 and the correlation were statistically significant at the 0.01 level. A 2nd-order random walk with topological adjacency, a structural-similarity-based biased walk (Ribeiro et al., 2017), and a deep learning-based trajectory simulation algorithm LSTM-TrajGAN (Rao et al., 2020) were also conducted as the baselines. The coefficient values were lower than our proposed algorithm. These results indicated that the proposed algorithm can capture the movement spatial pattern well. However, it is worth

Table 5
The correlation coefficients between the simulated trajectories and real trajectories.

Simulated algorithm	Number of stay points	Trajectory entropy	Crowd distribution	Interaction matrix
2nd-order – Movement	0.814**	0.809**	0.889**	0.903**
2nd-order – Topology	0.346**	0.555**	0.658**	0.606**
Structural-similarity-based	0.346**	0.538**	−0.158**	0.002**
LSTM-TrajGAN	−0.001	0.055**	0.041	0.011

** Correlation is significant at the 0.01 level.

noting that the simulation trajectories were still different from real trajectories. Therefore, we tried to find a balance between adding trajectories to address the sampling problem and reducing the noise. A model with simulation trajectories on all places was conducted for comparison. The RMSE, MAE, and StDev of this model were 8.951, 4.646, and 8.925, respectively, which was worse than those of our proposed method (as shown in Table 3). The ablation study results further demonstrated the effectiveness of our proposed trajectory enhancement algorithm. Furthermore, the performance difference between these two models is not that significant. This may be due to the fact that adding simulation trajectories in already crowded places has less effect on interaction modelling.

To further measure the multi-order spatial interaction effect on crowd distribution forecasting, a parameters analysis on the multi-order size and a spatial residual analysis were conducted. As shown in Fig. 11, the forecasting performance shows an overall trend of increasing and then decreasing with the increase in the multi-order interaction size and the best forecasting performance was achieved with the value of 9 (an RMSE of 8.885, MAE of 4.633, and standard deviation of error (StDev) of 8.884). This can be explained by the conjecture that a small size fails to capture the multi-order spatial interaction patterns, and a very large size results in too many places being considered, thus reducing the pertinence of modelling a specific place.

From the spatial perspective, the RMSE comparison between our proposed CDF-MSI method and the first-order interaction CDF-I method in each place was shown in Fig. 12. The places where the RMSE of CDF-I is greater than that of CDF-MSI were labelled in red, and the opposite parts were labelled in blue. Fig. 12(a) shows the overall comparison result across the country. It suggests that considering multi-order spatial interaction can improve forecasting performance on most places (CDF-I was significantly better than CDF-MSI on only 8.82 % of the places). The places where CDF-I performs better distributed sporadically. Combined with the local individual movement pattern, this may be explained by the fact that the lower frequency of movement among places of local residents reduces the impact of multi-order spatial interactions on the near real-time crowd distribution forecasting. Considering the greater application value of fine-grained crowd distribution forecasting in crowded areas, we selected region Dakar (where the capital of Senegal is located, marked as ①) and region Diourbel (one of the central core regions, marked as ②) to further analyse the differences in forecasting performance. It can be seen in Fig. 12(b) and 12(c) that our proposed method has achieved an overall advantage (CDF-I was significantly better than CDF-MSI on only 9.96 % and 3.97 % of places in Dakar and Diourbel, respectively), which demonstrated the superiority of considering the multi-order interaction in crowd distribution forecasting.

5. Discussion

5.1. Attempts at trajectory enhancement in interaction pattern learning

"How much data is big enough" is a typical but always overlooked problem in big data applications (Wang et al., 2017; Splinter et al., 2013). In these applications, we usually regard the acquired big data (sample) as a true reflection of the population, ignoring the impact of the chosen sampling strategy (e.g., the number of users and the time period) on the population characteristics. Especially in location-based transportation research, given the spatial heterogeneity phenomenon, sampling strategy differences can be particularly prominent in areas with sparse data. To explore the effect of crowd size on the sampling result, we randomly sampled 50 % of the trajectories from the dataset and generated the movement interaction matrixes of the post-sampling data and the pre-sampling data respectively. The experimental results showed that the correlation between the pre-sampling interaction matrix and the post-sampling interaction matrix in the crowded places was 0.93, while the correlation between the interaction matrix before and after sampling in the less crowded places was only 0.87. It indicated that the differences were mainly observed in the less crowded places. This situation exacerbated our concern with respect to modelling the interactions among the less crowded places using raw sample trajectory data. Data augmentation, which refers to methods for constructing sampling algorithms via the introduction of unobserved data, has been widely used in the fields such as language translation, image classification, and recommendation systems (Chen et al., 2019a,b; Van Dyk and Meng, 2001; Wang and Perez, 2017; Xie et al., 2020; Wang et al., 2020). For example, Chen et al. (2019) enriched the user-item network structure and employ node2vec to alleviate the data sparsity problem in recommender system. Wang et al. (2017) explored and compared multiple solutions to the problem of data augmentation in image classification. These studies implicated the potential of data augmentation in solving data sparsity problems. The trajectory enhancement algorithm was an instance of data augmentation in movement interaction pattern learning and an attempt to mitigate the insufficient sampling issue. Further explorations, such as more reasonable sampling expansion strategies or more diverse data, would contribute to a more comprehensive understanding of human movements and spatial interaction patterns.

5.2. The application of embedding learning techniques for multi-order spatial interaction learning

As the movements of individuals in space are continuous, the crowd distribution in a place is influenced by the surrounding places to a certain extent, thus reflecting the "coevolution" phenomenon. How to measure the spatial scope and intensity of this influence among different places has become an important topic for improving the accuracy of crowd distribution forecasting. Essentially, the influence among places originates from individual movements. Therefore, the inherent influence among places can be extracted from massive individual trajectories (Li et al., 2021; Liu et al., 2020; Liu et al., 2017).

A trajectory can be considered the combination of a series of stops and movements, which can be represented as a stop sequence such as "$location_1$, $location_2$, …, $location_k$". This means that the crowd distribution pattern of $location_w$ is influenced not only by $location_{h-1}$ and $location_{h+1}$ but also by locations from $location_{h-g}$ to $location_{h+g}$ (where g indicates the spatial scope of the influence mentioned in the above paragraph). This influence among multiple places was defined as a multi-order spatial interaction in this study.

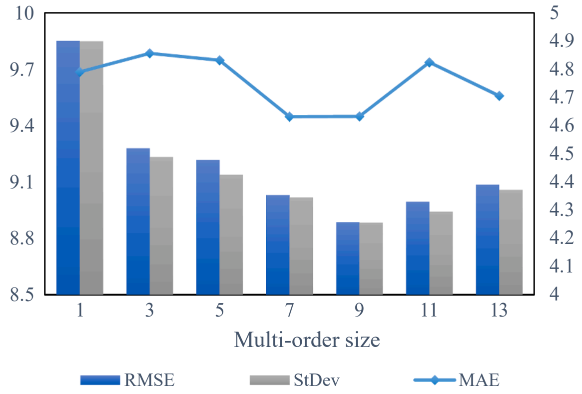

Fig. 11. Effect of the multi-order interaction size (RMSE and StDev using the left axis and MAE using the right axis).

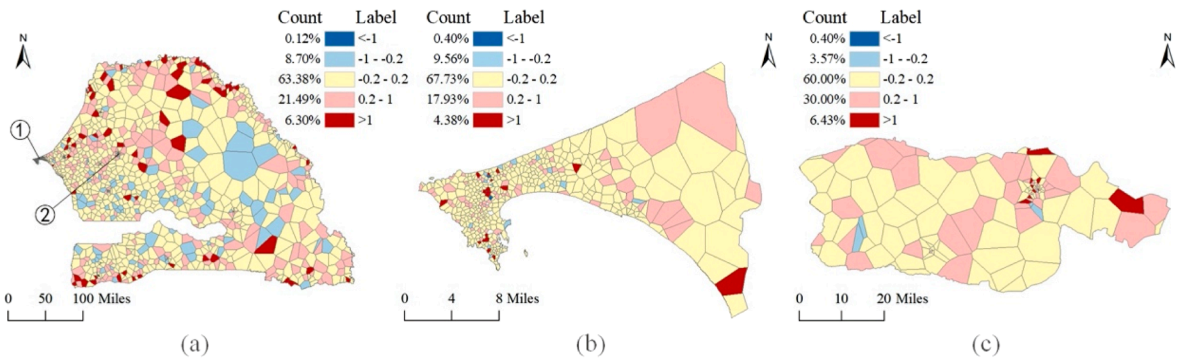

Fig. 12. Verification of multi-order interaction regarding RMSE (a) across the country (b) in region Dakar (c) in region Diourbel. The places labelled in blue indicate that the CDF-I performs better than CDF-MSI in these places. (For interpretation of the references to colour in this figure legend, the reader is referred to the web version of this article.)

The text-like structures of trajectories provide an efficient way to model the multi-order interaction among places using the embedding learning technique. Each location in the trajectory corresponding to the text structure "$word_1$, $word_2$, …, $word_k$" was analogous to a word in a sentence. Therefore, the multi-order spatial interactions can be regarded as the text similarity, which can be captured with embedding learning techniques. A higher multi-order spatial interaction intensity indicates that two places more frequently co-occur or possess common contextual neighbours in the trajectories, which also reflects higher spatial influence.

5.3. Limitations and future work

Several limitations of this study are worth noting and further exploring in future work. First, in the current CDF-MSI method, the 2nd-order random walk algorithm was used to generate simulated trajectories for trajectory data enhancement. Although this algorithm considered the historical movement pattern for transition weight matrix generation, the generated trajectories were still different from the real trajectories. This affected the accuracy and reliability of the spatial interaction modelling results to a certain extent. Advanced trajectory simulation strategies and other data expansion algorithms such as generative adversarial neural networks (Choi et al. 2021) and mobility Markov chain (Gambs et al. 2012) may further improve the forecasting performance. Second, the original word embedding model word2vec was applied in the proposed CDF-MSI method. This model can effectively extract the co-occurrence relationships and common context relationships among texts, which have been used in the explorations of road network structure (Chen et al., 2021; Wu et al., 2020; Wang et al., 2019). In our method, the multi-order spatial interactions among contextual non-adjacent places were modelled with this model using enhanced trajectories to capture the spatial correlations more comprehensively, thus improving the accuracy and stability of crowd distribution forecasting. It is worth noting that the implementation process in this paper has similarities with Node2Vec (Grover & Leskovec, 2016), but there are two differences. The initial weight matrix used in random walk of our method was based on the historical movement interaction, and the corresponding initial weight matrix of the Node2Vec was based on the topological adjacency. Besides, the Node2Vec method generates the same number of trajectories at each node, while our method does not. These made the learned edge weight matrix somewhat different. We also compared the forecasting performance based on our algorithm and the Node2Vec algorithm. The RMSE, MAE, and StDev of the Node2Vec based method were 9.528, 4.974, and 9.526, respectively, which was worse than those of our proposed method (8.885 on

RMSE, 4.633 on MAE, and 8.884 on StDev). Other advanced embedding learning techniques, such as BERT-flow and SimCSE, may help improve forecasting performance in future work (Su et al., 2021; Gao et al., 2021; Chen et al., 2021). In addition, the built environment can constrain and influence the movement behaviours of crowds (Tu et al., 2020). Five dimensions of the built environment (density, diversity, design, distance, and destination) were investigated for their effects on crowd distribution dynamics (Wu et al., 2018; Higgins & Kanaroglou, 2016). The consideration of the influence of the built environment can be an extension of crowd distribution forecasting methods. Moreover, it is worth noting that the network parameter has a great impact on forecasting performance. When increasing the number of GCN and LSTM layers from one to three, the RMSE of CDF-MSI model decreased from 8.885 to 8.589. Considering that the compared spatiotemporal graph-based models STMeta and ASTGCN typically used one spatial layer and one temporal layer for model training, we used one GCN layer and one LSTM layer in the case study to make the validation more comparable and less time consuming. The forecasting performance can be further improved by designing more complex network structures in future studies. Finally, in this study, the numbers of calls and mobile users were used to estimate the dynamic crowd distribution. Although linear relationships between crowd distribution and these two indicators have been demonstrated (Cheng et al., 2020; Kang et al., 2012), the potential impacts of sampling biases and uncertainty are of concern. Our future work will focus on solving these issues.

6. Conclusion

This study proposed a novel crowd distribution forecasting method considering the multi-order spatial interactions along different places using mobile phone data. We focus on two prevalent but not yet properly addressed limitations in current relevant studies: the insufficient interaction modelling in less crowded places caused by the lack of sampling design, and ignorance of multi-order spatial interactions among contextual non-adjacent places. To mitigate the influence of these issues, we applied a weighted random walk algorithm to generate simulated trajectories to improve the accuracy and robustness of the interaction characterizations in less crowded places. With the enhanced trajectories, we adopted an embedding learning algorithm to model the multi-order spatial interactions among contextual non-adjacent places. A hybrid forecasting model was then constructed that combines a GCN and an RNN for modelling the spatiotemporal pattern of crowd distribution variations. Our proposed method was verified using a real-world mobile phone dataset in a country. The results indicate that both the multi-order spatial interactions and the trajectory enhancement algorithm helped improve the crowd distribution forecasting performance. The CDF-MSI method also outperformed other baseline methods in terms of the RMSE, MAE, and StDev of the forecasting error.

This study provides an effective method to forecast fine-grained crowd distribution. The method allows us to capture future crowd distribution variations across space, which technically supports for transportation applications such as traffic optimization, emergency evacuation, and cell base station operation. In addition, crowd distribution variation patterns can help reveal the patterns of human movements, thus enriching the theory and practices related to human mobility studies.

CRediT authorship contribution statement

Mingxiao Li: Conceptualization, Methodology, Formal analysis, Visualization, Writing – original draft, Project administration. **Song Gao:** Conceptualization, Data curation, Investigation, Writing – review & editing. **Peiyuan Qiu:** Resources, Writing – review & editing. **Wei Tu:** Conceptualization, Resources, Writing – review & editing, Funding acquisition, Project administration. **Feng Lu:** Supervision, Resources, Writing – review & editing, Funding acquisition. **Tianhong Zhao:** Visualization, Writing – review & editing. **Qingquan Li:** Supervision, Resources, Writing – review & editing, Funding acquisition.

Declaration of Competing Interest

The authors declare that they have no known competing financial interests or personal relationships that could have appeared to influence the work reported in this paper.

Acknowledgement

This work is supported by the National Natural Science Foundation of China: [Grant No. 42101463, No. 42071360, No. 42271474, No. 71961137003]; the China Postdoctoral Science Foundation: [Grant No. 2021 M692164]; the Guangdong Province Basic and Applied Basic Research Fund Project: [Grant No. 2020A1515111166]; and a grant from State Key Laboratory of Resources and Environmental Information System.

Appendix A. Supplementary material

Supplementary data to this article can be found online at https://doi.org/10.1016/j.trc.2022.103908.

References

Aryal, G.R., 2020. Methods of Population Estimation and Projection. Journal of Population and Development 1 (1), 54–61.

Cecaj, A., Lippi, M., Mamei, M., & Zambonelli, F. 2020, June. Forecasting Crowd Distribution in Smart Cities. In 2020 IEEE International Conference on Sensing, Communication and Networking (SECON Workshops) (pp. 1-6). IEEE.

Chai, T., Draxler, R.R., 2014. Root mean square error (RMSE) or mean absolute error (MAE)?–Arguments against avoiding RMSE in the literature. Geosci. Model Dev. 7 (3), 1247–1250.

Chen, Y., Li, X., Cong, G., Bao, Z., Long, C., Liu, Y., Ellison, R., 2021. October). Robust Road Network Representation Learning: When Traffic Patterns Meet Traveling Semantics. In: In Proceedings of the 30th ACM International Conference on Information & Knowledge Management, pp. 211–220.

Chen, C., Ma, J., Susilo, Y., Liu, Y., Wang, M., 2016. The promises of big data and small data for travel behavior (aka human mobility) analysis. Transportation research part C: emerging technologies 68, 285–299.

Chen, J., Pei, T., Shaw, S.L., Lu, F., Li, M., Cheng, S., Zhang, H., 2018. Fine-grained prediction of urban population using mobile phone location data. International Journal of Geographical Information Science 32 (9), 1770–1786.

Chen, G., Viana, A.C., Fiore, M., Sarraute, C., 2019a. Complete trajectory reconstruction from sparse mobile phone data. EPJ Data Sci. 8 (1), 30.

Chen, J., Wu, Y., Fan, L., Lin, X., Zheng, H., Yu, S., Xuan, Q., 2019b. N2VSCDNNR: A local recommender system based on node2vec and rich information network. IEEE Trans. Comput. Social Syst. 6 (3), 456–466.

Chen, L., Liu, Y., He, X., Gao, L., Zheng, Z., 2019. Matching User with Item Set: Collaborative Bundle Recommendation with Deep Attention Network. In: IJCAI, pp. 2095–2101.

Cheng, S., Lu, F., Peng, P., 2020a. Short-Term Traffic Forecasting by Mining the Non-Stationarity of Spatiotemporal Patterns. IEEE Trans. Intell. Transp. Syst. https://doi.org/10.1109/TITS.2020.2991781.

Cheng, Z., Wang, J., Ge, Y., 2020b. Mapping monthly population distribution and variation at 1-km resolution across China. International Journal of Geographical Information Science 1–19. https://doi.org/10.1080/13658816.2020.1854767.

Choi, S., Kim, J., Yeo, H., 2021. TrajGAIL: Generating urban vehicle trajectories using generative adversarial imitation learning. Transportation Research Part C: Emerging Technologies 128, 103091.

Crivellari, A., Beinat, E., 2019. From motion activity to geo-embeddings: Generating and exploring vector representations of locations, traces and visitors through large-scale mobility data. ISPRS Int. J. Geo-Inf. 8 (3), 134.

Crols, T., Malleson, N., 2019. Quantifying the ambient population using hourly population footfall data and an agent-based model of daily mobility. GeoInformatica 23 (2), 201–220.

Cui, Z., Henrickson, K., Ke, R., Wang, Y., 2019. Traffic graph convolutional recurrent neural network: A deep learning framework for network-scale traffic learning and forecasting. IEEE Trans. Intell. Transp. Syst. 21 (11), 4883–4894.

De Montjoye, Y. A., Smoreda, Z., Trinquart, R., Ziemlicki, C., & Blondel, V. D. 2014. D4D-Senegal: the second mobile phone data for development challenge. arXiv preprint. arXiv:1407.4885.

Deville, P., Linard, C., Martin, S., et al., 2014. Dynamic population mapping using mobile phone data. PNAS 111 (45), 15888.

Friedman, J.H., 2001. Greedy function approximation: a gradient boosting machine. Ann. Stat. 1189–1232.

Gambs, S., Killijian, M.O., del Prado Cortez, M.N., 2012. Next place prediction using mobility markov chains. In: In Proceedings of the first workshop on measurement, privacy, and mobility, pp. 1–6.

Gao, S., 2015. Spatio-temporal analytics for exploring human mobility patterns and urban dynamics in the mobile age. Spatial Cognition & Computation 15 (2), 86–114.

Gao, T., Yao, X., & Chen, D. 2021. SimCSE: Simple Contrastive Learning of Sentence Embeddings. arXiv preprint arXiv:2104.08821.

Geng, X., Li, Y., Wang, L., Zhang, L., Yang, Q., Ye, J., Liu, Y., 2019. Spatiotemporal multi-graph convolution network for ride-hailing demand forecasting. In Proceedings of the AAAI conference on artificial intelligence 33 (1), 3656–3663.

Georganos, S., Grippa, T., Gadiaga, A., Vanhuysse, S., Kalogirou, S., Lennert, M., Linard, C., 2019. An application of geographical random forests for population estimation in Dakar, Senegal using very-high-resolution satellite imagery. In 2019 Joint Urban Remote Sensing Event. IEEE. 1–4 https://doi.org/10.1109/JURSE.2019.8809049.

Gonzalez, M.C., Hidalgo, C.A., Barabasi, A.L., 2008. Understanding individual human mobility patterns. Nature 453 (7196), 779–782.

Grover, A., & Leskovec, J. 2016. Node2vec: Scalable feature learning for networks. In Proceedings of the 22nd ACM SIGKDD International Conference on Knowledge Discovery and Data Mining (KDD '16). Association for Computing Machinery, New York, NY, USA, 855–864.

Guo, S., Lin, Y., Feng, N., Song, C., Wan, H., 2019. Attention based spatial-temporal graph convolutional networks for traffic flow forecasting. In Proceedings of the AAAI Conference on Artificial Intelligence 33, 922–929.

Gupta, R., Gozgor, G., Kaya, H., Demir, E., 2019. Effects of geopolitical risks on trade flows: evidence from the gravity model. Eurasian Economic Review 9 (4), 515–530.

Hara, H., Fujita, Y., Tsuda, K., 2020. Population estimation by random forest analysis using social sensors. Procedia Comput. Sci. 176, 1893–1902.

Higgins, C.D., Kanaroglou, P.S., 2016. A latent class method for classifying and evaluating the performance of station area transit-oriented development in the Toronto region. J. Transp. Geogr. 52, 61–72.

Hipp, J.R., Bates, C., Lichman, M., et al., 2018. Using social media to measure temporal ambient population: does it help explain local crime rates? Justice Q. 36 (4), 718–748.

Huang, B., Wang, J., Cai, J., Yao, S., Chan, P.K.S., Tam, T.H.W., Lai, S., 2021. Integrated vaccination and physical distancing interventions to prevent future COVID-19 waves in Chinese cities. Nat. Hum. Behav. https://doi.org/10.1038/s41562-021-01063-2.

Iacobucci, R., McLellan, B., Tezuka, T., 2019. Optimization of shared autonomous electric vehicles operations with charge scheduling and vehicle-to-grid. Transportation Research Part C: Emerging Technologies 100, 34–52.

Jin, G., Cui, Y., Zeng, L., Tang, H., Feng, Y., Huang, J., 2020. Urban ride-hailing demand prediction with multiple spatio-temporal information fusion network. Transportation Research Part C: Emerging Technologies 117, 102665. https://doi.org/10.1016/j.trc.2020.102665.

Kang, C., Liu, Y., Ma, X., Wu, L., 2012. Towards estimating urban population distributions from mobile call data. Journal of Urban Technology 19 (4), 3–21.

Ke, J., Feng, S., Zhu, Z., Yang, H., Ye, J., 2021. Joint predictions of multi-modal ride-hailing demands: A deep multi-task multi-graph learning-based approach. Transportation Research Part C: Emerging Technologies 127, 103063.

Krunić, N., Bajat, B., Kilibarda, M., 2015. Dasymetric mapping of population distribution in Serbia based on soil sealing degrees layer. In: Surface models for geosciences. Springer, Cham, pp. 137–149.

Leasure, D.R., Jochem, W.C., Weber, E.M., Seaman, V., Tatem, A.J., 2020. National population mapping from sparse survey data: A hierarchical Bayesian modeling framework to account for uncertainty. PNAS 117 (39), 24173–24179.

Li, Y., Yu, R., Shahabi, C., & Liu, Y. 2017. Diffusion convolutional recurrent neural network: Data-driven traffic forecasting. arXiv preprint arXiv:1707.01926.

Li, M., Gao, S., Lu, F., Zhang, H., 2019a. Reconstruction of human movement trajectories from large-scale low-frequency mobile phone data. Comput. Environ. Urban Syst. 77, 101346.

Li, M., Gao, S., Lu, F., Tong, H., Zhang, H., 2019b. Dynamic estimation of individual exposure levels to air pollution using trajectories reconstructed from mobile phone data. Int. J. Environ. Res. Public Health 16 (22), 4522.

Li, M., Zhang, H., Chen, J., 2019c. Fine-Grained Dynamic Population Mapping Method Based on Large-Scale Sparse Mobile Phone Data. In: In 2019 20th IEEE International Conference on Mobile Data Management (MDM). IEEE, pp. 473–478.

Li, M., Lu, F., Zhang, H., Chen, J., 2020. Predicting future locations of moving objects with deep fuzzy-LSTM networks. Transportmetrica A: Transport Science 16 (1), 119–136.

Li, M., Gao, S., Lu, F., Liu, K., Zhang, H., Tu, W., 2021. Prediction of human activity intensity using the interactions in physical and social spaces through graph convolutional networks. International Journal of Geographical Information Science 35 (12), 2489–2516.
Li, X., Pan, G., Wu, Z., Qi, G., Li, S., Zhang, D., Wang, Z., 2012. Prediction of urban human mobility using large-scale taxi traces and its applications. Frontiers of Computer Science 6 (1), 111–121.
Liang, V.C., Ma, R., Ng, W.S., Li, W., Zhang, Z., 2016. Mercury: Metro density prediction with recurrent neural network on streaming CDR data. In: In 2016 IEEE 32nd International Conference on Data Engineering (ICDE), pp. 1374–1377.
Liu, K., Gao, S., Qiu, P., Liu, X., Yan, B., Lu, F., 2017. Road2vec: Measuring traffic interactions in urban road system from massive travel routes. ISPRS Int. J. Geo-Inf. 6 (11), 321.
Liu, K., Gao, S., Lu, F., 2019. Identifying spatial interaction patterns of vehicle movements on urban road networks by topic modelling. Comput. Environ. Urban Syst. 74, 50–61.
Liu, Z., Ma, T., Du, Y., et al., 2018. Mapping hourly dynamics of urban population using trajectories reconstructed from mobile phone records. Transactions in GIS 22 (2), 494–513.
Liu, Y., Yao, X., Gong, Y., Kang, C., Shi, X., Wang, F., Zhu, X., 2020. Analytical methods and applications of spatial interactions in the era of big data. Acta Geographica Sinica 75 (7), 07001523.
Medrano, R.D., Aznarte, J.L., 2021. On the inclusion of spatial information for spatio-temporal neural networks. Neural Comput. Appl. https://doi.org/10.1007/s00521-021-06111-6.
Mellon, J., & Prosser, C. 2017. Twitter and Facebook are not representative of the general population: Political attitudes and demographics of British social media users. Research & Politics, 4(3), 2053168017720008.
Mikolov, T., Chen, K., Corrado, G., & Dean, J. 2013. Efficient estimation of word representations in vector space. In Proceedings of 1st International Conference on Learning Representations. Scottsdale, Arizona, USA, 1-12.
Mimura, T., Ishiguro, S., Kawasaki, S., Fukazawa, Y., 2019. Bike-share demand prediction using attention-based sequence to sequence and conditional variational autoencoder. In: Proceedings of the 3rd ACM SIGSPATIAL International Workshop on Prediction of Human Mobility, pp. 41–44.
Niu, X.Y., Ding, L., Song, X.D., 2015. Understanding Urban Spatial Structure of Shanghai Central City Based on Mobile Phone Data. China City Planning Review 24 (3), 15–23.
Ouyang, K., Liang, Y., Liu, Y., Tong, Z., Ruan, S., Rosenblum, D., Zheng, Y., 2020. Fine-grained urban flow inference. IEEE Trans. Knowl. Data Eng. https://doi.org/10.1109/TKDE.2020.3017104.
Panczak, R., Charles, E., Corcoran, J., 2020. Estimating temporary populations: a systematic review of the empirical literature. Humanities and Social Sciences Communications 6 (1), 1–10.
Park, H.J., Jo, W.S., Lee, S.H., Kim, B.J., 2018. Generalized gravity model for human migration. New J. Phys. 20 (9), 093018.
Park, C., Lee, J., Sohn, S.Y., 2019. Recommendation of feeder bus routes using neural network embedding-based optimization. Transportation Research Part A: Policy and Practice 126, 329–341.
Peng, H., Du, Y., Liu, Z., Yi, J., Kang, Y., Fei, T., 2019. Uncovering patterns of ties among regions within metropolitan areas using data from mobile phones and online mass media. GeoJournal 84 (3), 685–701.
Qiu, H., Zheng, Q., Msahli, M., Memmi, G., Qiu, M., Lu, J., 2020. Topological graph convolutional network-based urban traffic flow and density prediction. IEEE Trans. Intell. Transp. Syst. 22 (7), 4560–4569.
Rao, J., Gao, S., Kang, Y., & Huang, Q. 2020. LSTM-TrajGAN: A deep learning approach to trajectory privacy protection. arXiv preprint arXiv:2006.10521.
Ren, Y., Chen, H., Han, Y., Cheng, T., Zhang, Y., Chen, G., 2020. A hybrid integrated deep learning model for the prediction of citywide spatio-temporal flow volumes. Int. J. Geograph. Inf. Sci. 34 (4), 802–823.
Ribeiro, L.F., Saverese, P.H., Figueiredo, D.R., 2017. August). Struc2vec: Learning node representations from structural identity. In: In Proceedings of the 23rd ACM SIGKDD international conference on knowledge discovery and data mining, pp. 385–394.
Rumelhart, D.E., Hinton, G.E., Williams, R.J., 1986. Learning representations by back-propagating errors. Nature 323 (6088), 533–536.
Salat, H., Smoreda, Z., Schläpfer, M., 2020. A method to estimate population densities and electricity consumption from mobile phone data in developing countries. PLoS ONE 15 (6), e0235224.
Shaw, S.L., Yu, H.B., 2009. A GIS-based time-geographic approach of studying individual activities and interactions in a hybrid physical-virtual space. J. Transp. Geogr. 17 (2), 141–149.
Simini, F., González, M.C., Maritan, A., Barabási, A.L., 2012. A universal model for mobility and migration patterns. Nature 484 (7392), 96–100.
Smith, B.L., Williams, B.M., Oswald, R.K., 2002. Comparison of parametric and nonparametric models for traffic flow forecasting. Transport. Res. Part C: Emerg. Technol. 10 (4), 303–321.
Splinter, K.D., Turner, I.L., Davidson, M.A., 2013. How much data is enough? The importance of morphological sampling interval and duration for calibration of empirical shoreline models. Coast. Eng. 77, 14–27.
Stathakis, D., Baltas, P., 2018. Seasonal population estimates based on night-time lights. Comput. Environ. Urban Syst. 68, 133–141.
Stouffer, S.A., 1940. Intervening opportunities: a theory relating mobility and distance. Am. Sociol. Rev. 5 (6), 845–867.
Su, J., Cao, J., Liu, W., & Ou, Y. 2021. Whitening sentence representations for better semantics and faster retrieval. arXiv preprint arXiv:2103.15316.
Tobler, W., 1976. Spatial interaction patterns. Journal of Environmental Systems 6 (4), 271–301.
Tu, W., Zhu, T., Xia, J., Zhou, Y., Lai, Y., Jiang, J., Li, Q., 2020. Portraying the spatial dynamics of urban vibrancy using multisource urban big data. Comput. Environ. Urban Syst. 80, 101428.
Ullman, E.L., 1953. Human geography and area research. Ann. Assoc. Am. Geogr. 43 (1), 54–66.
Van Dyk, D.A., Meng, X.L., 2001. The art of data augmentation. Journal of Computational and Graphical Statistics 10 (1), 1–50.
Wang, J., Dong, L., Cheng, X., Yang, W., Liu, Y., 2019b. An extended exploration and preferential return model for human mobility simulation at individual and collective levels. Phys. A 534, 121921.
Wang, L., Chai, D., Liu, X., Chen, L., & Chen, K. 2020. Exploring the Generalizability of Spatio-Temporal Crowd Flow Prediction: Meta-Modeling and an Analytic Framework. arXiv preprint arXiv:2009.09379.
Wang, M.X., Lee, W.C., Fu, T.Y., Yu, G., 2019c. Learning embeddings of intersections on road networks. In: In Proceedings of the 27th ACM SIGSPATIAL International Conference on Advances in Geographic Information Systems, pp. 309–318.
Wang, H., Li, L., Pan, P., Wang, Y., Jin, Y., 2019a. Early warning of burst passenger flow in public transportation system. Transportation Research Part C: Emerging Technologies 105, 580–598.
Wang, W., Liu, C., Zhao, D., 2017. How much data are enough? A statistical approach with case study on longitudinal driving behavior. IEEE Trans. Intell. Veh. 2 (2), 85–98.
Wang, J., Perez, L., 2017. The effectiveness of data augmentation in image classification using deep learning. Convolutional Neural Networks Vis. Recognit 11, 1–8.
Wang, D., Zhong, W., Yin, Z., Xie, D., Luo, X., 2018. Spatio-temporal dynamics of population in shanghai: A case study based on cell phone signaling data. In: Big Data Support of Urban Planning and Management. Springer, Cham, pp. 239–254.
World Bank. (2014). World Development Indicators. Available at: http://data.worldbank.org/country. Accessed May 17, 2021.
Wu, Y., Tan, H., Qin, L., Ran, B., Jiang, Z., 2018. A hybrid deep learning based traffic flow prediction method and its understanding. Transportation Research Part C: Emerging Technologies 90, 166–180.
Wu, N., Zhao, X.W., Wang, J., Pan, D., 2020. Learning effective road network representation with hierarchical graph neural networks. In: In Proceedings of the 26th ACM SIGKDD International Conference on Knowledge Discovery & Data Mining, pp. 6–14.
Xie, Q., Dai, Z., Hovy, E., Luong, T., Le, Q., 2020. Unsupervised data augmentation for consistency training. Advances in Neural Information Processing Systems 33, 6256–6268.

Xing, X., Huang, Z., Cheng, X., Zhu, D., Kang, C., Zhang, F., Liu, Y., 2020. Mapping Human Activity Volumes Through Remote Sensing Imagery. IEEE J. Sel. Top. Appl. Earth Obs. Remote Sens. 13, 5652–5668.
Xu, Y., Belyi, A., Bojic, I., Ratti, C., 2018. Human mobility and socioeconomic status: Analysis of Singapore and Boston. Comput. Environ. Urban Syst. 72, 51–67.
Xu, Z., Hou, L., Zhang, Y., Zhang, J., 2022. Passenger Flow Prediction of Scenic Spot Using a GCN-RNN Model. Sustainability 14 (6), 3295.
Xu, J., Rahmatizadeh, R., Bölöni, L., Turgut, D., 2017. Real-time prediction of taxi demand using recurrent neural networks. IEEE Trans. Intell. Transp. Syst. 19 (8), 2572–2581.
Xue, F., Cao, Y., Ding, Z., Tang, H., Yang, X., Chen, L., et al., 2020. Urban population density estimation based on spatio-temporal trajectories. Concurrency and Computation: Practice and Experience 32 (14), e5685.
Yang, X., Fang, Z., Xu, Y., Yin, L., Li, J., Lu, S., 2019. Spatial heterogeneity in spatial interaction of human movements—Insights from large-scale mobile positioning data. J. Transp. Geogr. 78, 29–40.
Yao, X., Gao, Y., Zhu, D., Manley, E., Wang, J., Liu, Y., 2020. Spatial Origin-Destination Flow Imputation Using Graph Convolutional Networks. IEEE Trans. Intell. Transp. Syst. https://doi.org/10.1109/TITS.2020.3003310.
You, H., Jin, C., Sun, W., 2020. Spatiotemporal evolution of population in northeast China during 2012–2017: a nighttime light approach. Complexity 2020, 1076–2787.
Yuan, Y., Raubal, M., 2016. Analyzing the distribution of human activity space from mobile phone usage: an individual and urban-oriented study. International Journal of Geographical Information Science 30 (8), 1594–1621.
Zhang, J., Zheng, Y., Qi, D., 2017. Deep spatio-temporal residual networks for citywide crowd flows prediction. In Proceedings of the AAAI Conference on Artificial Intelligence 31 (1), 1655–1661.
Zhang, J., Chen, F., Guo, Y., Li, X., 2020a. Multi-graph convolutional network for short-term passenger flow forecasting in urban rail transit. IET Intel. Transport Syst. 14 (10), 1210–1217.
Zhang, Y., Cheng, T., Ren, Y., Xie, K., 2020b. A novel residual graph convolution deep learning model for short-term network-based traffic forecasting. International Journal of Geographical Information Science 34 (5), 969–995.
Zhang, J., Li, X., Yao, Y., Hong, Y., He, J., Jiang, Z., Sun, J., 2021. The Traj2Vec model to quantify residents' spatial trajectories and estimate the proportions of urban land-use types. International Journal of Geographical Information Science 35 (1), 193–211.
Zhang, G., Zhu, A.X., 2018. The representativeness and spatial bias of volunteered geographic information: a review. Ann. Gis 24 (3), 151–162.
Zhen, F., Qin, X., Ye, X., Sun, H., Luosang, Z., 2019. Analyzing urban development patterns based on the flow analysis method. Cities 86, 178–197.
Zheng, C., Fan, X., Wang, C., Qi, J., 2020. GMAN: A graph multi-attention network for traffic prediction. In Proceedings of the AAAI Conference on Artificial Intelligence 34 (01), 1234–1241.
Zhu, D., Huang, Z., Shi, L., Wu, L., Liu, Y., 2018. Inferring spatial interaction patterns from sequential snapshots of spatial distributions. International Journal of Geographical Information Science 32 (4), 783–805.
Zhu, H., Xie, Y., He, W., Sun, C., Zhu, K., Zhou, G., Ma, N., 2020a. A novel traffic flow forecasting method based on RNN-GCN and BRB. Journal of Advanced Transportation. https://doi.org/10.1155/2020/7586154.
Zhu, D., Zhang, F., Wang, S., Wang, Y., Cheng, X., Huang, Z., Liu, Y., 2020b. Understanding Place Characteristics in Geographic Contexts through Graph Convolutional Neural Networks. Annals of the American Association of Geographers 110 (2), 408–420.
Zipf, G.K., 1946. The PJVD hypothesis on the intercity movement of persons. Am. Sociol. Rev. 11, 677–686.